www.czasopisma.pan.pl PAN POLSKA AKADEMIA NAUK www.journals.pan.pl

Arch. Metall. Mater., Vol. 61 (2016), No 2B, p. 1221–1227

DOI: 10.1515/amm-2016-0202

T. RATAJSKI*#, I. KALEMBA-REC*, B. DUBIEL*

MANUFACTURING, MICROSTRUCTURE AND CORROSION RESISTANCE OF ELECTROPHORETICALLY DEPOSITED SiO_2 AND Ni/SiO_2 COATINGS ON X2CrNiMo17–12–2 STEEL

The SiO_2 and Ni/SiO_2 coatings were electrophoretically deposited on X2CrNiMo17-12-2 steel using ethanol-based suspensions of the SiO_2 and Ni powders. The influence of the zeta potential and concentration of the suspensions, the applied voltage and deposition time on the quality of the coatings was studied. Microstructure of the plan-view and cross sections of the coatings was investigated using scanning electron microscopy. The plan-view images revealed the uniform microstructure of the coatings with sporadically observed cracks, pores as well SiO_2 and Ni agglomerates. On the cross-sections, the Cr_2O_3 layer, resulted from oxidation of the substrate during sintering of the coatings was observed. The polarization tests have shown that SiO_2 and Ni/SiO_2 coatings improve the corrosion resistance of the X2CrNiMo17-12-2 steel in 3.5% NaCl aqueous solution.

Keywords: electrophoretic deposition (EPD), SiO_2 coatings, nancomposite Ni/SiO_2 coatings

1. Introduction

Due to the high corrosion resistance, the X2CrNiMo17-12-2 austenitic stainless steel is frequently used for application in atmospheric conditions, acids environments and in the presence of some salts [1]. However, in Cl^- containing solutions, such as seawater, chlorinated water or physiological fluids, this steel undergoes pitting and crevice corrosion [2]. The susceptibility to localised corrosion can be reduced by application of coatings or corrosion inhibitors [3]. Very promising protective properties are offered by ceramic and composite coatings. Several types of ceramic coatings have been developed. The most pronounced improvement of corrosion resistance was obtained by application of oxide coatings, such as Al_2O_3, ZrO_2-CeO_2, Zr_2O_3, SiO_2, TiO_2, Cr_2O_3 [4-9]. The overall quality and properties of the coatings can differ significantly depending on used deposition technique. A great number of innovative treatments of oxide coatings are nowadays under investigation. In the literature such methods as plasma detonation technique [10], arc-ion plating [11], sol-gel deposition [12-13], chemical conversion layers of cerium [14] and chromium [15], chemical vapor deposition (CVD) [16], high-velocity oxy-fuel spray [17], plasma-nitriding [18], atomic layer deposition (ALD) [19, 20] and electrophoretic deposition (EPD) [21] are reported. Between them, EPD is a very promising method that allows deposition of high-quality coatings of various materials at room temperature in comparatively short time.

Among many ceramic coatings, SiO_2 is widely used due to its good corrosion and wear resistance as well as high hardness. The corrosion resistance of the SiO_2 coatings on austenitic stainless steel deposited by EPD from aqueous suspensions was investigated by Castro et al. [22]. They have confirmed that the silica coatings act as effective barriers for corrosion in sea-water. As it was reported by Atik and Aegerter [6], SiO_2 coatings on X2CrNiMo17-12-2 stainless steel improve also corrosion resistance in 15% H_2SO_4 environment.

High resistance to pitting and crevice corrosion can be also obtained by using nanocomposite nickel matrix coatings [23]. Ni composite coatings, containing inorganic non-metal nanoparticles as the reinforcing phase, find wide applications requiring anti-corrosion, anti-wear and anti-friction properties [24]. The combinations that have received considerable attention are nickel with SiC, SiO_2, TiO_2, ZrO_2 and Al_2O_3 nanoparticles [25-29]. Among the nanoparticles used for reinforcement, SiO_2 is frequently studied and applied due to its high hardness, good oxidation resistance and good chemical stability. The two main techniques, which are used for deposition of nickel matrix composites, are the electrodeposition [25] and electroless deposition [27]. Both types of deposition techniques require use of harmful baths. There are also some reports indicating the possibility of combination of nickel electrodeposition with electrophoretic deposition of silica particles [30-31]. In all cases, increasing nanoparticle content in the nanocomposite improves the corrosion resistance of the coating. The corrosion potential of such composite in 3.5% NaCl solution decreases up to – 0.3 V in comparison with the nickel coating.

There is still a limited number of publications providing the information about possibility of effective application of elec-

* AGH UNIVERSITY OF SCIENCE AND TECHNOLOGY, FACULTY OF METALS ENGINEERING AND INDUSTRIAL COMPUTER SCIENCE, AL. A MICKIEWICZA 30, 30-059 KRAKOW, POLAND

Corresponding author: ratajski@agh.edu.pl

trophoretic deposition technique for manufacturing of Ni/SiO_2 composite coatings [32].

Electrophoretic deposition is a traditional processing method in the ceramic industry that is gaining increasing interest for production of new materials coatings. EPD is achieved through the movement of charged particles dispersed in a suitable liquid towards an electrode under an applied electric field. This movement results in the accumulation of the particles and in the formation of a homogeneous deposit at the appropriate electrode [33]. The biggest advantages of EPD method are the uniformity of received coatings and the possibility of controlling process parameters. Thanks this technique one can control also the deposition rate.

The aim of this work was to determine the optimum parameters of the electrophoretic deposition of SiO_2 and Ni/SiO_2 coatings on X2CrNiMo17-12-2 stainless steel as well as to examine their microstructure and corrosion resistance in aqueous 3.5% NaCl solution.

2. Materials and methods

For electrophoretic deposition of SiO_2 and Ni/SiO_2 coatings ethanol-based suspensions were used. Spherical SiO_2 nanoparticles with diameter from 10 nm to 40 nm and nickel particles with diameter from 160 nm to 650 nm were delivered by SIGMA-ALDRICH.

The substrate for deposition of the coatings was X2CrNiMo17-12-2 stainless steel, known also as AISI 316L grade, cut for the rectangular plates 15 mm width × 30 mm length × 0.5 mm thick. The nominal chemical composition of the steel is as follows (wt %): 0.03 C, 18 Cr, 14 Ni, 2.8 Mo, 2 Mn, 0.2 Si, 0.03 S, 0.045 P. The samples were grinded with sandpaper of 2000 grit and then cleaned with distilled water and ethanol.

For electrophoretic deposition of the SiO_2 coatings, suspensions containing different concentrations of nanopowder in the range of 0.8 g/L – 1.6 g/L in ethanol were used. In the case of the nanocomposite Ni/SiO_2 coatings, the similar suspensions additionally containing 1.5 g of Ni powder were prepared.

To disperse powders as well as to prevent aggregation and settling of the particles, the suspensions were placed in ultrasonic bath for 40 minutes and then stirred for one hour. For SiO_2 suspensions the magnetic stirrer was used. Due to the ferromagnetic properties of Ni, for the Ni/SiO_2 suspensions the mechanical stirring was carried out. For determination of the suspension stability the zeta potential of particles is very important. When the zeta potential reaches large absolute values, the particles repel each other and thus the suspension is stable. In opposite, when the zeta potential is low, the particles coagulate [34]. pH and zeta potential of suspensions were measured by means of Mettler Toledo pH meter and Malvern Zetasizer Nano ZS90, respectively. The changes of suspensions pH were realized by addition of acetic acid or NaOH. In order to select the optimum conditions for coatings deposition, these experiments were carried out using constant applied voltage in the range 5-50 V and deposition time varied from 60 s to 420 s. After EPD the samples were dried at room temperature and annealed at temperature 800°C for 15 minutes in air (SiO_2 coatings) or in argon (Ni/SiO_2 nanocomposite coatings). Macroscopic investigation of the coatings quality was focused on observation of such defects like an uneven thickness, cracks and voids.

Microstructural investigation was carried out by means of scanning electron microscopes (SEM) FEI Nova NanoSEM 450 and JEOL Neoscope II JCM-6000 using plan view and cross-section specimens. For transmission electron microscopy (TEM) analysis the thin lamellas were prepared by Focused Ion Beam (FIB) method using FEI QUANTA 3D 200i. TEM investigation was performed using JEOL JEM-2010ARP microscope. Microanalysis of chemical composition was carried out by means of energy dispersive X-ray spectroscopy (EDS).

The corrosion resistance of coated and uncoated specimens in 3.5% NaCl solution was investigated by polarization test using Autolab Potentiostat/Galvanostat PGSTAT302N. The measurements were carried out with use of platinum counter electrode at the potential range from – 0.5 V to + 0.5 V and scan rate 0.005 V/s.

3. Results and discussion

3.1. Selection of the EPD parameters

The electrophoretic deposition depends on parameters related to the suspensions and to the physical conditions of the process. The trial coatings were deposited using suspensions with different concentrations of SiO_2 and Ni powders. The macroscopic inspection showed that the most uniform coatings were deposited from suspensions of 1.2 g/L of SiO_2 and 1.2 g/L of SiO_2+ 1.5 g of Ni in ethanol. To examine the stability of suspensions, the influence of pH on zeta potential was investigated.

Figure 1 shows the relationship between zeta potential and pH for suspensions of SiO_2, Ni as well as both SiO_2 and Ni particles in ethanol. For suspension containing 1.2 g/L SiO_2 nanoparticles in ethanol it was found, that the isoelectric point occurs when the pH value is equal to 5.2. For higher pH, the absolute value of zeta potential is growing and thus the stability of the suspension increases. When the pH is equal to 6.97, the zeta potential reaches the value of -11.6 mV. For higher pH, despite the rise of zeta potential, the inhomogeneous coatings were deposited. Therefore, for deposition of SiO_2 coatings the suspension with pH of 6.97 was selected. As the silicon oxide particles exhibit negative charge in ethanol solutions, they were electrophoretically deposited on anode.

In case of co-deposition of different materials, namely metallic Ni and ceramic SiO_2 particles, it was necessary to find a suitable pH value, for which the both substances are deposited on the same electrode. Therefore, in order to select the parameters for electrophoretic deposition of Ni/SiO_2 coatings, the measurements of zeta potential versus pH were carried out for suspensions of Ni particles as well as both SiO_2 and Ni particles

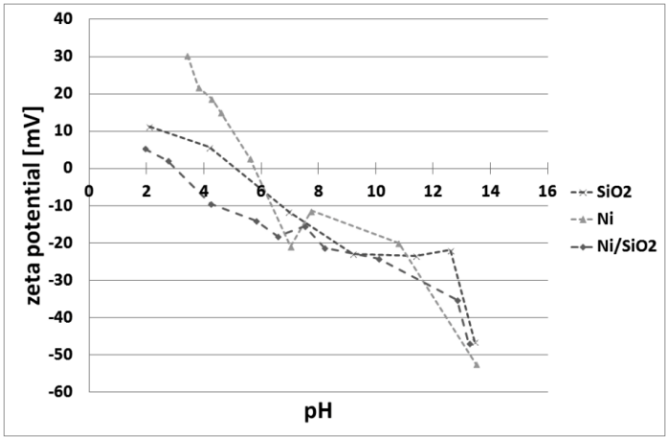

Fig. 1. Relationship between zeta potential and pH for suspensions of SiO_2, Ni as well as both SiO_2 and Ni particles in ethanol

in ethanol. It can be seen in (Fig. 1), that the isoelectric point for Ni suspension is equal to 5.78. It means, that in the pH range from 5.70 to 5.80 the charges of the SiO_2 and Ni particles in ethanol are opposite.

The zeta potential function versus pH obtained for the mixture of powders is more similar in its shape to the function determined for SiO_2, rather than Ni. The isoelectric point is shifted to more acidic range, as compared with solutions of SiO_2 or Ni, and occurs at pH equal to 3.0. For higher values of pH the zeta potential is negative. For pH larger than 8.21, despite an increase of the absolute value of zeta potential, deterioration of the quality of the coatings surface was observed. Therefore, pH value of the suspension used for preparation of the Ni/SiO_2 coatings was equal to 8.21.

The best quality coatings with macroscopically uniform thickness and free from voids and cracks were obtained for solution containing 1.2 g/L SiO_2 in ethanol at the applied constant voltage of 30 V and deposition time equal to 180 s (Fig. 2a).

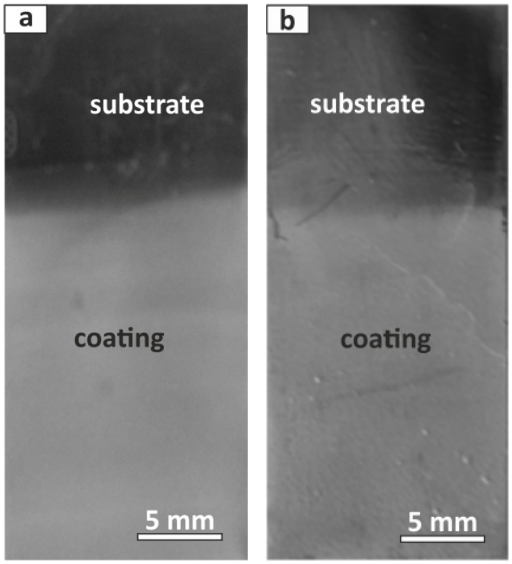

Fig. 2. Macroscopic images of SiO_2 (a) and Ni/SiO_2 (b) coatings deposited using applied voltage equal to 30 V and time equal to 180 s

For such conditions the relationship between the deposit mass on the area unit and the deposition time was determined (Fig. 3a). Assuming, that the function of area density versus time is linear, it was estimated that the speed of deposition was 0.04 mg/cm^2×s.

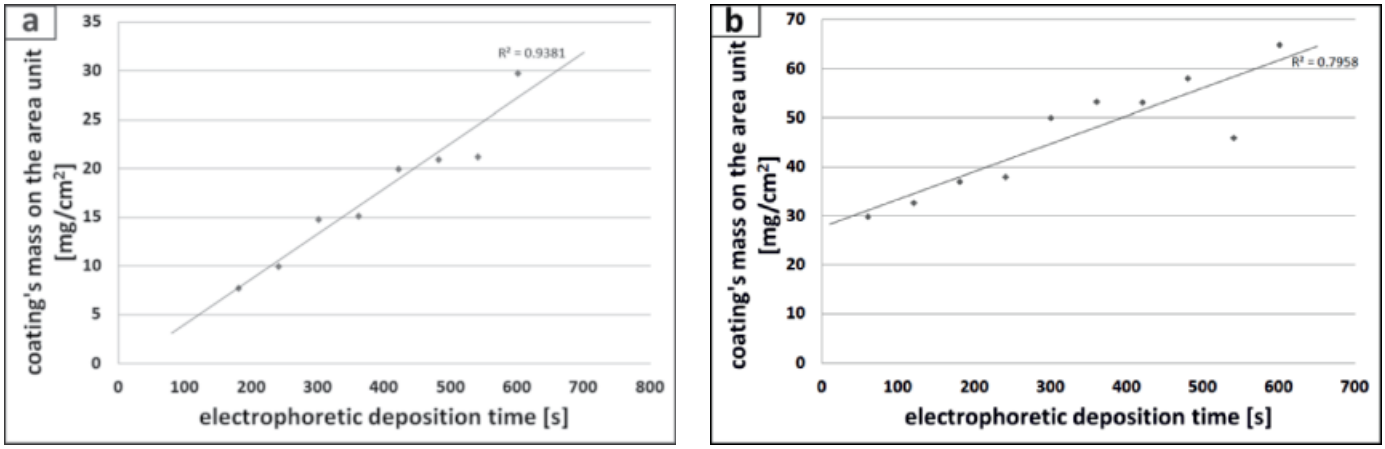

Fig. 3. Relationship between SiO_2 (a) and Ni/SiO_2 (b) coating's mass on the area unit and electrophoretic deposition time

Based on the macroscopic inspection it was found, that the most homogeneous coatings were produced using applied voltage equal to 30 V and deposition time equal to 3 minutes (Fig. 2b). Relationship between the area density of the coating and the deposition time was also examined (Fig. 3b). The results show good agreement with the linear function. The estimated speed of deposition was 0.056 mg/cm^2×s.

3.2. Microstructure of SiO_2 coatings

Microstructural investigation of plan view specimens using SEM showed that the coatings are homogenously deposited on the substrate. The small cracks and pores as well as aggregations of silica nanoparticles 1-2 μm in size were observed (Fig. 4a). The nature of cracks indicates that the possible reason of their

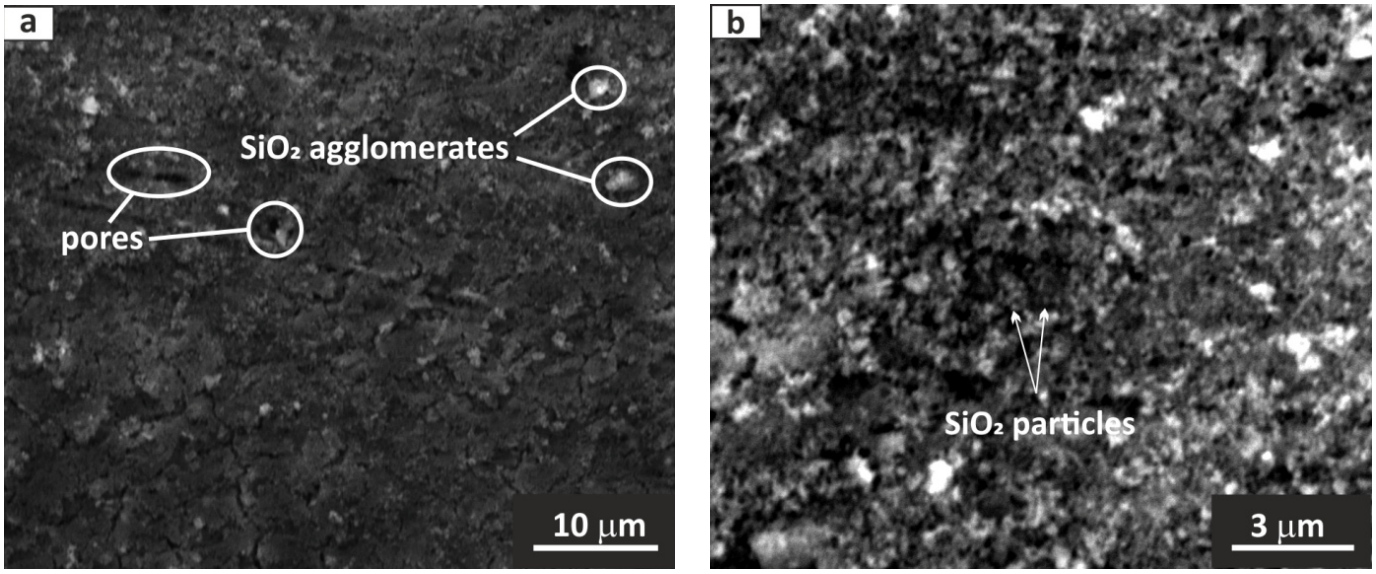

Fig. 4. Microstructure of the surface of the SiO_2 coating on the X2CrNiMo17-12-2 steel after electrophoretic deposition and annealing at temperature 800°C for 15 minutes, plan view SEM images: (a) the view of the area showing the distribution of agglomerates and pores, (b) the sintered SiO_2 particles within the coating

formation is the silica shrinkage during drying. The images acquired at higher magnification show the tightly adherent sintered spherical SiO_2 particles (Fig. 4b).

SEM microstructural investigation and EDS microanalysis of the chemical composition on the cross-section specimens revealed, that between substrate and SiO_2 coating the layer of chromium oxide was present (Fig. 5). The thickness of SiO_2 coatings was in the range from 1.6 μm to 2.5 μm, while the thickness of the Cr_2O_3 layer varied from 0.9 μm to 1.3 μm. It can be concluded that oxidation of the steel surface occurs during annealing due to the discontinuities in the coatings in the form of cracks and pores. TEM microstructural investigation of the cross-section sample shown that the electrophoretically deposited SiO_2 coating is composed from nanolayers of densely packed particles, separated by the less tightly adherent rows containing nanopores (Fig. 6).

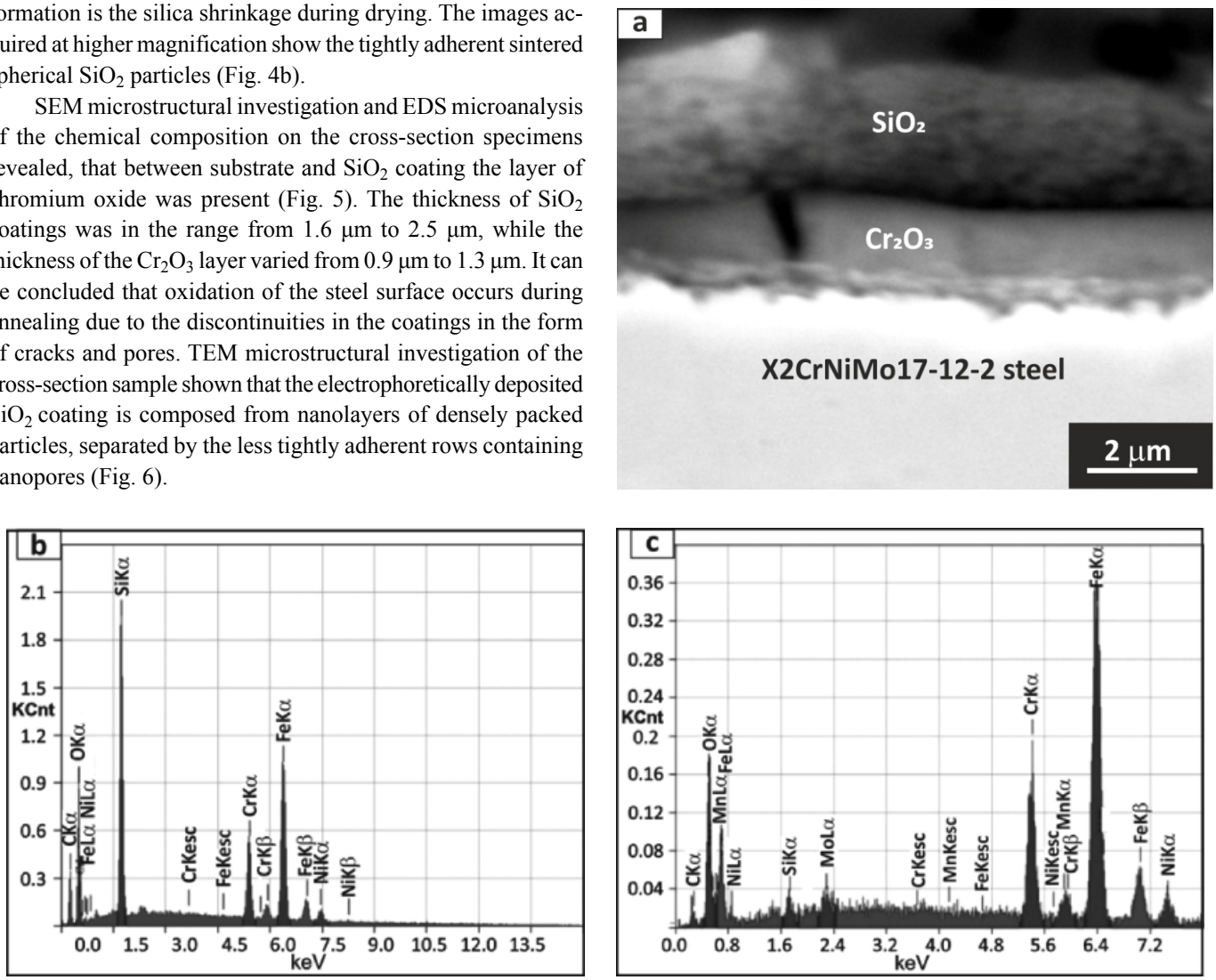

Fig. 5. a) SEM image of the cross-section of SiO_2 coating on X2CrNiMo17-12-2 steel and EDS spectra from SiO_2 coating (b) and Cr_2O_3 oxide layer (c)

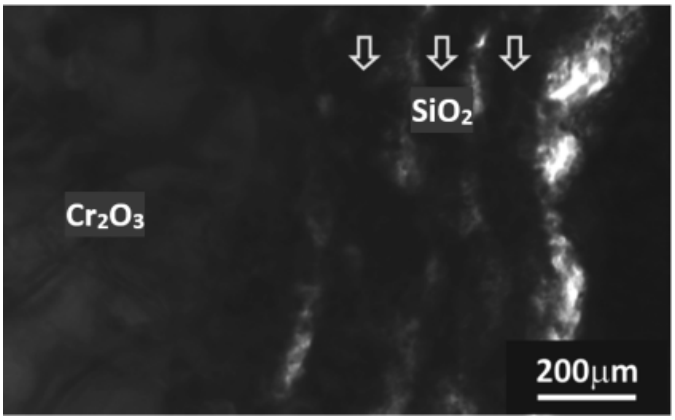

Fig. 6. TEM image of the cross-section showing the layered microstructure of the SiO_2 coating and underlying Cr_2O_3 formed on X2CrNiMo17-12-2 steel substrate

3.3. Microstructure of the Ni/SiO_2 coating

SEM investigation revealed, that the coating was characterized by high homogeneity. The SiO_2 and Ni particles were uniformly distributed and the bonding between them was strong. Sporadically, some agglomerates of SiO_2 and Ni were present (Fig. 7).

SEM analysis of the microstructure performed using cross-section specimen showed, that the thickness of Ni/SiO_2 coating on stainless steel substrate was in the range of 2.5 μm – 3 μm (Fig. 8a). Despite the use of protective atmosphere of argon during annealing, the presence of chromium oxide on the steel surface was observed. The oxide scale was discontinuous with numerous cracks. Its thickness varied from 0.98 μm to 1.89 μm.

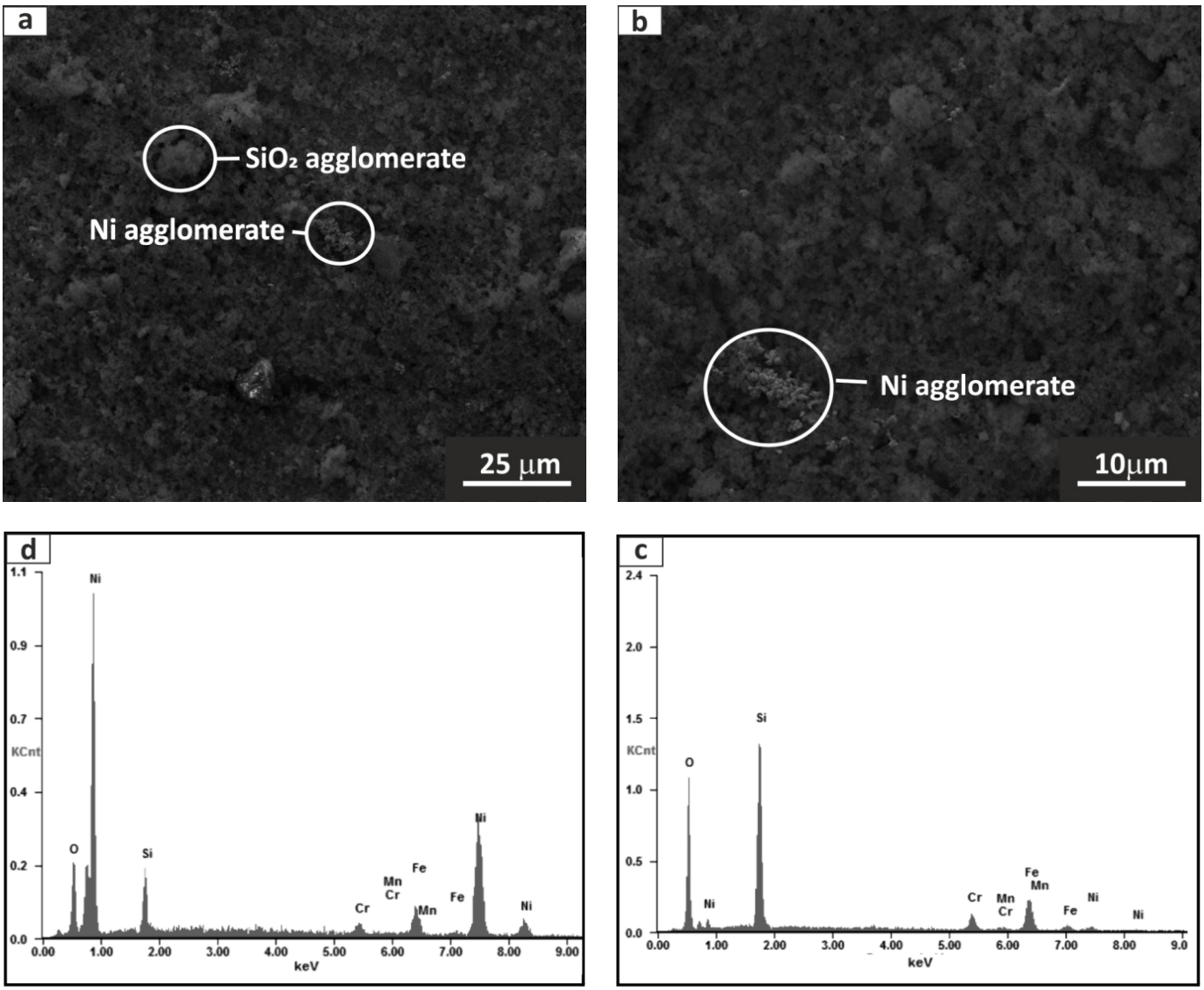

Fig. 7. Microstructure of the surface of the Ni/SiO_2 coating on the X2CrNiMo17-12-2 steel after electrophoretic deposition and annealing at temperature 800°C for 15 minutes, plan view SEM images: (a) the view of the area showing the distribution of agglomerates, (b) the spherical SiO_2 particles within the coating and EDS spectra from SiO_2 (c) and Ni agglomerates (d)

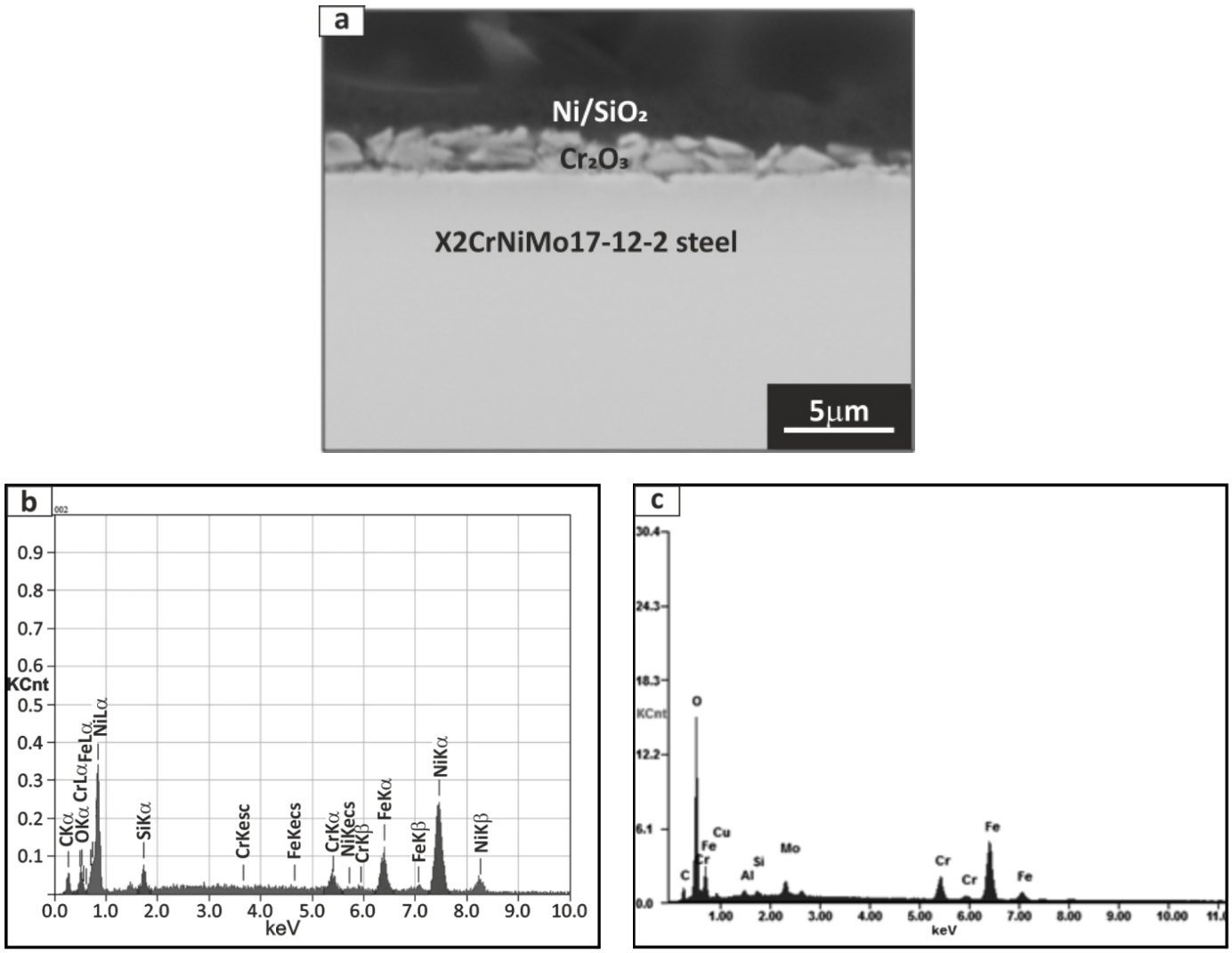

Fig. 8. SEM image of the cross-section of Ni/SiO_2 coating on X2CrNiMo17-12-2 steel (a) and EDS spectra from Ni/SiO_2 coating area (b) and Cr_2O_3 oxide layer (c)

3.4. Corrosion resistance

The corrosion resistance of the samples was determined by means of polarization test in 3.5% NaCl aqueous solution. Figure 9 shows anodic polarization curves for uncoated X2CrNiMo17-12-2 steel and coated by SiO_2 and Ni/SiO_2.

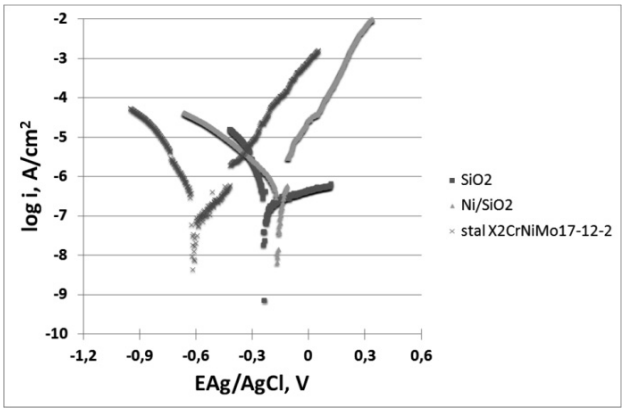

Fig. 9. Polarization curves for X2CrNiMo17-12-2 steel without coatings as well as with SiO_2 and Ni/SiO_2 coatings

The corrosion potential for coated steel is shifted to more positive values with respect to the corrosion potential of steel without coatings (E_{corr} = –0.6 V). The best corrosion resistance shows the steel coated with Ni/SiO_2 nanocomposite (E_{corr} = –0.17 V). Corrosion potential (E_{corr}) of the SiO_2 coated steel is equal to E_{corr} = –0.23 V.

Based on the SEM analysis of the cross-sections of the coated steel, it can be confirmed that the Ni/SiO_2 composite coating exhibits relatively small amount of cracks and good adhesion to the substrate, what influences the better protection against permeation of Cl^- ions. In case of SiO_2 coating the occurrence of cracks and pores is more pronounced. This may be the reason why the more compact Ni/SiO_2 coating exhibits slightly better corrosion resistance.

It was reported in [30] that addition of SiO_2 nanoparticles increases the corrosion resistance of nickel coatings obtained by electrodeposition. The corrosion potential of the austenitic stainless steel with electrodeposited Ni/SiO_2 coatings can be increased up to –0.28 V in 3.5% NaCl solution [35], what is a little lower as for the electrophoretically deposited coating achieved in the present work.

4. Conclusions

1) Based on the obtained results it can be concluded that EPD is a convenient method to produce ceramic and nanocomposite corrosion resistant coatings on stainless steel substrate.
2) The optimized conditions for the electrophoretic deposition of the SiO_2 and Ni/SiO_2 coatings were selected. The best quality coatings were obtained using constant applied voltage of 30 V and deposition time of 3 minutes. The SiO_2 coatings were deposited from 1.2 g/L suspension with zeta potential equal to –11.6 mV. The Ni/SiO_2 coatings were deposited at zeta potential equal to –21.3 mV and the concentration of the suspension was 1.2 g/L of SiO_2 + 1.5 g/L of Ni.
3) The microstructure of achieved coatings was relatively homogeneous with sparsely distributed cracks and pores. Some agglomerates of SiO_2 and Ni were observed. In order to deposit coatings without agglomerates, further optimisation of EPD process is required.
4) After sintering, the presence of Cr_2O_3 oxide under the coatings was observed on the SEM images of the cross-section samples. Oxidation of the steel substrate occurred during annealing and was related with the discontinuities of the coatings.
5) SiO_2 and Ni/SiO_2 coatings prepared by electrophoretic deposition method are characterized by very good corrosion resistance in 3.5% NaCl aqueous solution.

Acknowledgements

The work was supported by the statutory project of AGH-UST no. 11.11.110.293. The authors would like to thank Dr. Marta Gajewska for preparation of the sample by FIB in the Academic Center of Materials and Nanotechnology AGH.

The authors kindly acknowledge the company JEOL (EUROPE) SA branch in Poland for allowing access to the JEOL electron microscope JCM-6000 NeoScope II for this investigation.

REFERENCES

[1] M. Blicharski, Inżynieria Materiałowa. Stal, Warszawa 2004.
[2] S. Atashin, M. Pakshir, A. Yazdani, Mater. Design. **32**, 1315-1324 (2011).
[3] L. Adamczyk, A. Piertusiak, H. Bala, Arch. Metall. Mater. **56**, 883-889 (2011).
[4] I.N. Reddy, V.R. Reddy, N. Sridhara, V.S. Rao, M. Bhattacharya, P. Bandyopadhyay, [5] S. Basavaraja, A.K. Mukhopadhyay, A.K. Sharma, A. Dey, Ceram. Int. **40**, 9571-9582 (2014).
[6] R. Di Maggio, L. Fedrizzi, S. Rossi, P. Scardi, Thin Solid Films. **286**, 127-135 (1996).
[7] M. Atik, M.A. Aegerter, J. Non-Cryst. Solids. **147-148**, 813-819 (1992).
[8] M. Atik, P. De Lima Neto, L.A. Avaca, M.A. Aegerter, J. Zarzycki, J. Mater. Sci. Lett. **13**, 1081-1085 (1994).
[9] L. Curkovic, H. Otmacic-Curkovic, S. Salopek, M. Majic-Renjo, S. Šegota, Corros. Sci. **77**, 176-184 (2013).
[10] C.R. Tomachuk, C.I. Elsner, A.R. Di Sarli, O.B. Ferraz, Mater. Chem. Phys. **119**, 19-29 (2010).
[11] E. Marin, L. Guzman, A. Lanzutti, W. Ensinger, L. Fedrizzi, Thin Solid Films. **522**, 283-288 (2012).
[12] C. Liu, G. Lin, D. Yang, M. Qi, Surf. Coat. Technol. **200**, 142-147 (2006).
[13] V.H.V. Sarmento, M.G. Schiavetto, P. Hammer, A.V. Benedetti, C.S. Fugivara, P.H. Suegama, S.H. Pulcinelli, C.V. Santilli, Surf. Coat. Technol. **204**, 2689-2701 (2010).
[14] R. Di Maggio, L. Fedrizzi, S. Rossi, P. Scardi, Thin Solid Films. **286**, 127-135 (1996).
[15] C. Wang, F. Jiang, F. Wang, Corros. Sci. **46**, 75-84 (2004)
[16] C.R. Tomachuk, C.I. Elsner, A.R. Di Sarli, O.B. Ferraz, Mater. Chem. Phys. **119**, 19-29 (2010).
[17] D. Pech, P. Steyer, J.P. Millet, Corros. Sci. **50**, 1492-1497 (2008).
[18] J. Kawakita, T. Fukushima, S. Kuroda, T. Kodama, Corros. Sci. **44**, 2561-2581 (2002).
[19] C.X. Li, T. Bell, Corros. Sci. **48**, 355-361 (2006).
[20] B. Díaz, J. Światowska, V. Maurice, A. Seyeux, B. Normand, E. Härkönen, M. Ritala, P. Marcus, Electrochem. Acta. **28**, 10516-10523 (2011).
[21] E. Marin, A. Lanzutti, L. Guzman, L. Fedrizzi, J. Coat. Technol. Res. **5**, 655-659 (2011).
[22] R. Hayashi, M. Yamamoto, K. Tsunetomo, K. Kohno, Y. Osaka, H. Nasu, Jpn. J. Appl. Phys. **129**, 756-761 (1990).
[23] Y. Castro, B. Ferrari, R. Moreno, A. Duran, Surf. Coat. Tech. **191**, 228-235 (2005).
[24] J. Sudagar, J. Lian, W. Sha, J. Alloys Compd. **571**, 183–204 (2013).
[25] B. Bakhit, A. Akbari, F. Nasirpouri, M.G. Hosseini, Appl. Surf. Sci. **307**, 351-359 (2014).
[26] S. Sadreddini, A. Afshar, Appl. Surf. Sci. **303**, 125-130 (2014).
[27] T.R. Tamilarasan, R. Rajendran, G. Rajagopal, J. Sudagar, Surf. Coat. Tech. **276**, 320-326 (2015).
[28] J.A. Calderon, J.E. Henao, M.A. Gomez, Electrochem. Acta. **124**, 190-198 (2014).
[29] E. Bełtowska-Lehman, A. Góral, P. Indyka, Arch. Metall. Mater. **56**, 919-931 (2011).
[30] W. Sassi, L. Dhouibi, P. Bercot, M Rezrazi, Appl. Surf. Sci. **324**, 369-379 (2015).
[31] Y. Wang, Q. Zhou, K. Li, Q. Zhong, Q.B. Bui, Ceram. Int. **41**, 79-84 (2015).
[32] A. Ghalayani Isfahani, M. Ghorbani, J. Nano. Res. **26**, 45-51 (2014).
[33] J.H. Dickerson, Aldo R. Boccaccini, Electrophoretic deposition of nanoparticles, Springer, 2012.
[34] L. Besra, M. Liu, Prog. Mater. Sci. **52**, 1-61 (2007).
[35] T. Rabizadeh, S.R. Allahkaram, Mater. Design. **32**, 133-138 (2011).